The Influence of High Sound Speed Confinement on Detonation Propagation in High Explosives

Mark Short, Carlos Chiquete, Stephen J. Voelkel
Shock and Detonation Physics, Los Alamos National Laboratory,
Los Alamos, NM 87545, USA

1 Introduction

Detonations in conventional high explosives (HEs) typically travel at speeds of 6-8 mm/μs, have reaction zone lengths on the order of 100s of micrometers to a couple of millimeters, and can generate pressures in the range of 30-40 GPa through the reaction zone. In contrast, detonations in non-ideal HEs have typical detonation speeds in the range 3-5 mm/μs, reaction zone lengths on the order of millimeters to centimeters, and can generate pressures in the range of 5-10 GPa. The propagation of detonation in an HE is significantly influenced by the properties of the surrounding confinement, which affects the structure of detonation driving zone (DDZ) [1]. The following work concerns confinement by an inert material whose sound speed is either much greater than, or of the order of, the Chapman-Jouguet (CJ) detonation speed.

Eden and Belcher [2] studied the detonation and confiner wave-shapes in a 2D planar slab geometry, where an insensitive TATB-based HE (EDC-35) was confined by beryllium (Be), whose sound speed ($\approx$ 8 mm/μs) is comparable to the CJ detonation speed of the HE. Weak precursor elastic waves in the Be ran ahead of the detonation front at the Be sound speed, while a larger amplitude wave in the Be was seen to ride just ahead of the detonation front. They also observed a structure attributed to either a shock or lateral Be surface movement into the HE generated by this large amplitude Be wave. Detonation front shapes in the non-ideal HE ANFO (CJ speed $\approx$ 4.8 mm/μs) confined by aluminum (sound speed 5.3 mm/μs) for varying HE and Al thicknesses were studied by Jackson, Kiyanda and Short [3]. Some evidence of a turn up in the detonation wave shape is evident near the Al confiner. Also, Short and Jackson [4] have shown that the detonation speed in a fixed width of ANFO increases significantly as the Al confiner wall thickness is increased. Moreover, the outer Al confinement wall expansion profiles show a smooth rise in time, indicating the lack of any shock waves in the Al confinement material.

By imposing a detonation wave pressure loading along the HE-confiner interface, Sharpe and Bdzil [5] obtained theoretical insights into the confiner flow when the detonation speed (D_0) is lower than the confiner sound speed (c_M). Their analysis considered the limit where changes in the inert sound speed are small (sufficiently strong confiner). The resulting confiner flow depended on two parameters, namely the wall thickness relative to the detonation reaction zone width, and the magnitude of the difference between D_0 and c_M. It was found that the HE-confiner interface is deflected into the HE ahead of the detonation, with the magnitude of the inward deflection increasing either as the wall thickness increased,

Correspondence to: short1@lanl.gov

or as the difference between D_0 and c_M increased. Sharpe and Bdzil [5] conjectured that in certain circumstances, the detonation could be driven up to speeds approaching the confiner sound speed.

Short *et al.* [6] presented numerical simulations of a model for non-ideal HE detonation confined by Al, where $D_{CJ} < c_M$. The detonation phase speed was observed to be driven up close to the CJ value, supported by the lateral deflection of the inner Al wall into the explosive ahead of the detonation. Sharpe *et al.* [7] studied detonation confinement with $D_{CJ} = c_M$. They observed that if the outer confiner boundary was rigid, i.e. unable to expand, then, in certain circumstances depending on the confiner properties, the detonation speed D_0 could be driven above c_M.

2 Model

For the high pressures induced by detonation loading, we model the flow in both the explosive and confiner with the compressible Euler equations [1],

$$\frac{D\rho}{Dt} + \rho\nabla\cdot\mathbf{u} = 0, \quad \frac{D\mathbf{u}}{Dt} = -\frac{1}{\rho}\nabla p, \quad \frac{De}{Dt} = \frac{p}{\rho^2}\frac{D\rho}{Dt}, \tag{1}$$

for density ρ, pressure p, particle velocity $\mathbf{u} = (u, v)$ and specific internal energy e. The material derivative $D/Dt = \partial/\partial t + \mathbf{u}\cdot\nabla$, where t is time.

For the HE, we use a stiffened-gas condensed-phase detonation model [1], whereupon the equation of state (EOS) model for the internal energy, e, the specific reaction enthalpy of the HE, q, and the frozen sound speed, c, are given by

$$e = \frac{p+A}{(\gamma-1)\rho} - q\lambda, \quad q = \frac{D_{CJ}^2}{2(\gamma^2-1)}\left(1 - \frac{A}{\rho_0 D_{CJ}^2}\right)^2, \quad c = \left[\frac{\gamma p + A}{\rho}\right]^{1/2}, \tag{2}$$

respectively, where γ is the adiabatic exponent, A is the stiffened gas constant, ρ_0 is the initial density of the HE and D_{CJ} is the Chapman-Jouguet (CJ) speed. Also, λ is the reaction progress variable ($0 \le \lambda \le 1$). The associated reaction model is

$$\frac{D\lambda}{Dt} = kp^n(1-\lambda)^\nu, \tag{3}$$

where k is a rate constant, n is the pressure exponent and ν is a reaction order variable. Reference scales are given in [8], where the reference length scale is the length behind the shock in the steady, planar Chapman-Jouguet detonation wave at which half of the reactant has been consumed. For a typical insensitive HE we take [1], $\rho_0 = 2$, $A = 12.8$, and $D_{CJ} = 8$, while for a typical non-ideal HE [1] we take $\rho_0 = 0.86$, $A = 0$, $D_{CJ} = 4.8$. We also choose the equation-of-state and weakly state-sensitive rate parameters [1], $\gamma = 3$, $n = 1$, and $\nu = 1/2$.

For the confiner layer region, we use a Mie-Grüneisen EOS with a reference curve that is based on a linear shock speed (U_s) - particle speed (u_p) Hugoniot-state variation, where $U_s = c_c + su_p$ [1]. Here c_c is the sound speed at the ambient state, while s is the slope dU_s/du_p. The corresponding internal energy of the Mie-Grüneisen EOS is

$$e = \frac{c_c^2\sigma^2}{2(1-s\sigma)^2} + \frac{1}{\Gamma_{c0}\rho_{c0}}\left(p - \frac{\rho_{c0}c_c^2\sigma}{(1-s\sigma)^2}\right), \ \sigma = 1 - \frac{\rho_{c0}}{\rho}, \tag{4}$$

where Γ_{c0} is the Grüneisen gamma and ρ_{c0} is the ambient confiner density. For the current work, we consider beryllium (Be). It has a density of 1.85 g/cm^3 and a high sound speed of 7.99 mm/μs. With the

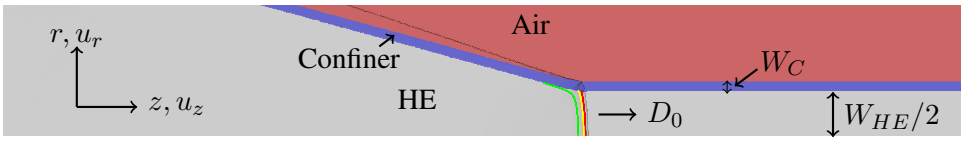

Figure 1: A section of a typical 2D planar. multi-material computational geometry showing HE (light grey), confiner (blue) and air (red) regions.

nondimensionalisation [8], the EOS parameters for Be [1] are given by $c_c = 7.99$, $s = 1.13$, $\rho_{c0} = 1.85$, and $\Gamma_0 = 2$.

A section of the typical 2D planar computational geometry under consideration is shown in Fig. 1, where HE is confined by Be, and where $\mathbf{x} = (r, z)$, $\mathbf{u} = (u_r, u_z)$. Outside of the confiner is an air layer, so that the confiner can expand laterally. This region is modeled with an ideal gas EOS $\tilde{e} = \tilde{p}/(\gamma_a - 1)\tilde{\rho}$, $\gamma_a = 1.4$, where the initial air density is $\rho_{a0} = 0.0012$. Symmetry conditions are applied along the bottom boundary of Fig. 1, so that for a total HE height W_{HE}, the HE region shown has height $W_{HE}/2$. The confiner thickness is W_C. The channel length L in varied to ensure steady state propagation is obtained. Outflow conditions are applied along the left, right and top boundaries. The detonation wave in the HE is initiated by placing a quarter-circle region of radius $W_{HE}/4$ at the CJ pressure in the left bottom corner of the HE region.

The flow equations in the HE, confiner and air regions are integrated with a cell-centered finite volume method on a Cartesian mesh within the multi-material simulation framework AMRITA-MultiMat. A second-order minmod spatial reconstruction with a Lax-Friedrichs flux is used together with a second-order total variation diminishing Runge-Kutta time integration. Material interfaces are treated with a Ghost Fluid method using a linearized Riemann solution closure [9], and evolved using a level set strategy. A block structured adaptive-mesh-refinement capability is also employed. For the computations below, two levels of refinement are used with a refinement factor of four for each level. The resolution of the finest grid is specified by the number of points (Npts) per the unit (half-reaction zone) length defined above. A resolution of Npts $= 80$ was used.

3 Confiner sound speed larger than the CJ speed

We first examine the effect of detonation in the non-ideal HE model confined by Be, where D_{CJ} (4.8) is significantly smaller than the Be sound speed (7.99). Figure 2L shows the variation of axial detonation speed D_0 with varying Be thickness for $W_{HE} = 15$ and 30. There is a significant increase in D_0 as the Be thickness increases for both HE widths. In particular, for sufficiently thick Be, D_0 is driven significantly above the theoretical maximum self-sustaining value D_{CJ}. Of particular interest is that D_0 for the thinner HE increases above that of the thicker HE as W_c increases.

Figure 2R shows the local detonation and confiner flow structure for $W_c = 120$ and $W_{HE} = 15$ through a weighted pressure gradient image, a case previously described in [1]. The phase speed is $D_0 \approx 5.8$ mm/μs, so that $c_M > D_0$, and thus the confiner has no shock polar solution in a frame traveling with the detonation. Correspondingly, the flow in the confiner is observed to be entirely subsonic and shockless (Fig. 2R). A large amplitude confiner pressure disturbance lies ahead of the detonation, coupled to the propagating detonation. The pressure disturbance consists of a set of waves radiating axially and laterally from a region near the detonation front intersection with the material interface The waves decay as they propagate away from the region, with the wavehead propagating at c_M. The pressure built up in the confiner causes a lateral expansion of the wall back into the HE both ahead of the detonation and for most of the reaction zone (Fig. 3). The material flow expansion in the HE due to reaction

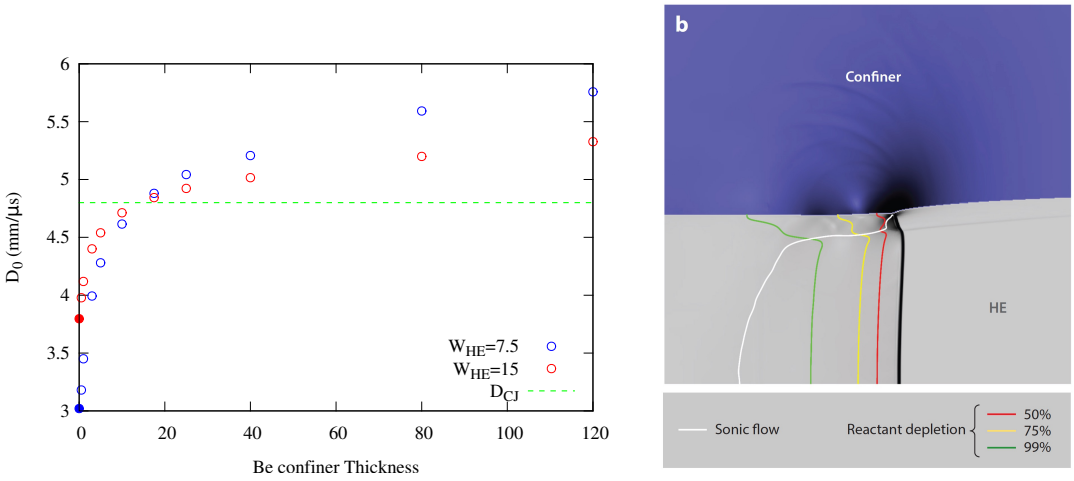

Figure 2: Left (L): Detonation speed variation D_0 with Be layer thickness for the non-ideal HE model with $W_{HE} = 15$ (blue) and 30 (red). Right (R): Weighted pressure gradient image of the detonation and confiner flow structure for $W_c = 120$ and $W_{HE} = 15$ (from [1]).

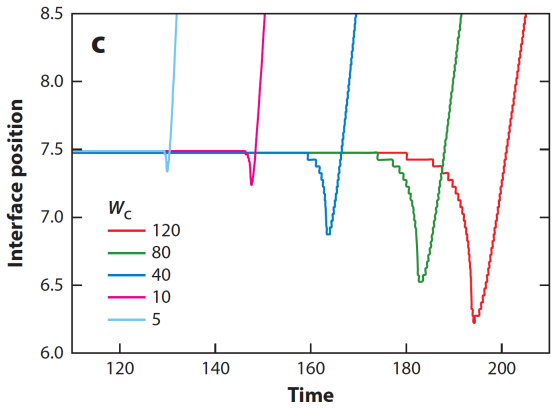

Figure 3: Deflection of the HE/Be interface in time for various Be confiner thicknesses along a fixed axial location for $W_{HE} = 15$ (from [1]).

subsequently pushes the confiner wall back out. Although a significant part of the detonation front is convergent (Fig. 2R), a sonic locus still exists in the HE. This is behind the reaction zone in the bulk of the charge. The sonic line defining the DDZ intersects the material boundary close to the detonation shock. Thus, the flow along the material boundary is supersonic on the HE side. The fact that the confiner flow is subsonic and allows information to flow ahead of the detonation pushing the interface into the HE, underlies how the confiner thickness and its material properties have a significant influence on D_0 and the DDZ structure. All cases in Fig. 2L have a basic flow structure similar to that shown in Figs. 2R and 3, but the extent and magnitude of the flow in the Be layer is significantly affected by the Be thickness.

If the HE is surrounding by a weak confiner, such as an elastomer (El), the detonation propagation is unaffected by the material properties of the confinement [1]. The sonic layer in the DDZ intersects the detonation shock at the the HE/confiner boundary. Given the strong effect that a Be layer has on detonation propagation, it is of interest to examine how the placement of an El layer between the HE and Be affects detonation propagation. Multilayer confinement has been examined in [10], but not for

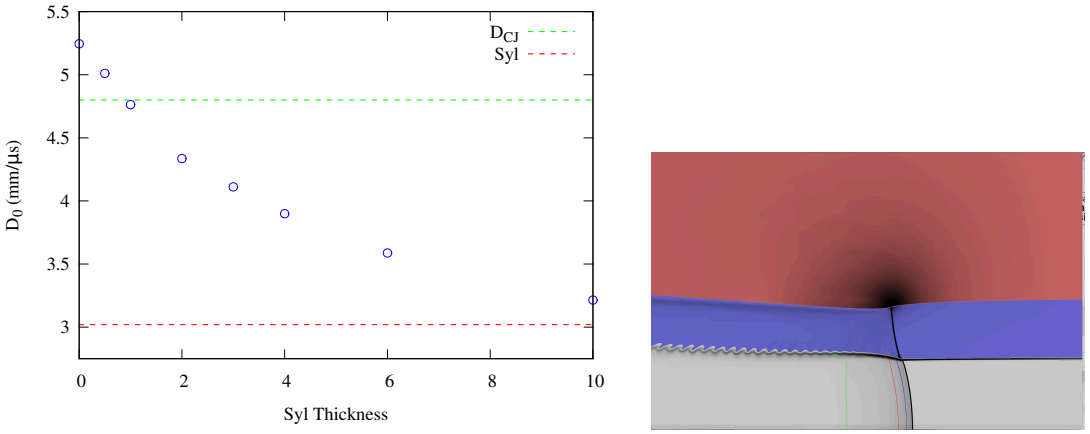

Figure 4: (L) Detonation speed variation D_0 with El layer thickness for the non-ideal HE model with $W_{HE} = 15$ and Be thickness $W_c = 40$. (R) Weighted pressure gradient image of the detonation and confiner flow structure for $W_c = 40$, $W_{HE} = 15$ and El thickness $W_{El} = 6$. Note, due to the addition of the El layer into the simulation, here the El layer is shown in blue, while the Be layer is in red.

a high sound speed outer confinement layer. The El EOS model has $c = 1.127$, $s = 1.2$, $\Gamma_0 = 1.5$, and $\rho_0 = 0.5$ [1]. Figure 4L shows the variation of D_0 with increasing El layer thickness for the non-ideal HE model above with $W_{HE} = 15$ and $W_c = 40$. As the El layer thickness increases, D_0 drops below D_{CJ} and for sufficient thick El layers, asymptotes toward the unconfined speed. Figure 4R shows a weighted pressure gradient image of the detonation and confiner flow structure for $W_c = 40$, $W_{HE} = 15$ and El thickness 6. The detonation shock is now divergent, whereas without the El layer it is convergent. However, the shock transmitted into the El is convergent. The flow in the Be layer is again shockless and subsonic, and connected to the HE layer by the El layer shock. Similar to Fig 2R, in the Be layer, there is a pressure disturbance consisting of a set of waves radiating axially and laterally from a region near where the El shock intersects the Be layer. However, its effect on the detonation structure is weakened by having to transmit its presence through the El layer.

4 Comparable confiner sound speed and CJ speed

The next case we examine is for the insensitive HE model where $D_{CJ} = 8$, so that D_{CJ} is close to the Be sound speed. Figure 5L shows the detonation speed variation D_0 with Be thickness for $W_{HE} = 20$. With no Be confinement, D_0 is significantly lower that D_{CJ} due to curvature effects in the narrow channel size. As the Be layer width increases, D_0 increases, reaching D_{CJ} for $W_c \approx 25$. Up to this point, the flow in the Be is subsonic and shockless. As the Be width increases further, D_0 increases above D_{CJ}, and a leading shock wave develops in the Be layer. A weighted pressure gradient image of the detonation and confiner flow structure for $W_c = 40$ is shown in Fig. 5R. The confiner flow now consists of a complex of supersonic and subsonic wave structures. In particular, near the detonation front, there is a subsonic high pressure regime that radiates pressure outward, in a similar manner to the non-ideal HE case above. However, the flow is now bounded by the lead shock wave in the Be. The detonation front is convergent.

5 Summary

We have examined how detonation propagation in an idealized non-ideal or insensitive HE is affected by confinement by an inert material whose sound speed is greater than, or of the order of, the Chapman-

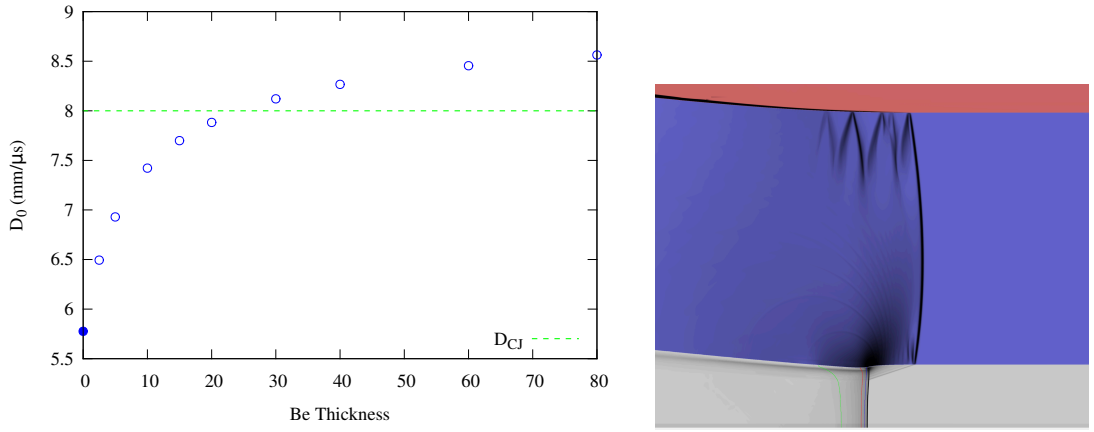

Figure 5: (L) Variation of D_0 with Be thickness for the insensitive HE model with $W_{HE} = 20$. (R) Weighted pressure gradient image of the detonation and confiner flow for $W_c = 40$ and $W_{HE} = 20$.

Jouguet (CJ) detonation speed. We have highlighted the complex flow structures that arise in the coupling between the HE detonation and confiner, and the major effect this has on the detonation speed.

References

[1] M. Short and J.J. Quirk. High explosive detonation-confiner interactions. *Annu. Rev. Fluid Mech.*, 50:215–242, 2018.

[2] G. Eden and R.A. Belcher. The effects of inert walls on the velocity of detonation in EDC35, an insensitive high explosive. In *Ninth Symposium (International) on Detonation*, pages 831–841. Office of the Chief of Naval Research, 1989.

[3] S.I. Jackson, C.B. Kiyanda, and M. Short. Experimental observations of detonation in ammonium-nitrate-fuel-oil (ANFO) surrounded by a high-sound speed, shockless, alumium confiner. *Proc. Combust. Instit.*, 33(2):2219–2226, 2011.

[4] M. Short and S.I. Jackson. Dynamics of high sound-speed metal confiners driven by non-ideal high-explosive detonation. *Combust. Flame*, 162:1857–1867, 2015.

[5] G.J. Sharpe and J.B. Bdzil. Interactions of inert confiners with explosives. *J. Eng. Math.*, 54:273–298, 2006.

[6] M. Short, J.J. Quirk, C.K. Kiyanda, S.I. Jackson, M.E. Briggs, and M.A. Shinas. Simulation of detonation of ammonium nitrate fuel oil mixture confined by aluminium: Edge angles for DSD. In *Fourteenth International Detonation Symposium*, pages 769–778. Office of Naval Research, 2010.

[7] G.J. Sharpe, M.Y. Luheshi, M. Braithwaite, and S.A.E.G. Falle. Steady non-ideal detonation. In *AIP Conference Proceedings*, volume 1195, pages 452–457. American Institute of Physics, 2009.

[8] M. Short, J.J. Quirk, C. Chiquete, and C.D. Meyer. Detonation propagation in a circular arc: reactive burn modelling. *J. Fluid Mech.*, 835:970–998, 2018.

[9] J.J. Quirk. amr_sol::multimat. Technical Report LA-UR-07-0539, Los Alamos National Laboratory, Los Alamos, NM, USA, 2007.

[10] M. Short, C. Chiquete, and J.J. Quirk. The influence of multi-layer confinement on detonation propagation in condensed-phase explosives. *Proc. Combust. Instit.*, 38:3595–3603, 2021.